DALTON
FULL PAPER

Phosphine containing dendrimers for highly regioselective rhodium catalysed hydroformylation of alkenes: a positive 'dendritic effect' †

Loïc Ropartz,[a] Katherine J. Haxton,[a] Douglas F. Foster,[b] Russell E. Morris,*[a] Alexandra M. Z. Slawin[a] and David J. Cole-Hamilton*[a]

[a] *School of Chemistry, University of St. Andrews, St. Andrews, Fife, Scotland, UK KY16 9ST*
[b] *Catalyst Evaluation and Optimisation Service (CATS), School of Chemistry, University of St. Andrews, St. Andrews, Fife, Scotland, UK KY16 9ST*

Received 8th July 2002, Accepted 4th September 2002
First published as an Advance Article on the web 1st November 2002

Diphenylphosphine functionalised polyhedral oligomeric silsesquioxane (POSS) dendrimers are used as ligands for the rhodium catalysed hydroformylation of oct-1-ene showing unexpectedly high regioselectivity to the linear aldehyde nonan-1-al (l : b = 14 : 1). Comparative studies with the small molecule analogues, bis-diphenylphosphinopentane, $Me_2Si[CH_2CH_2PPh_2]_2$ and $Si[CH_2CH_2PPh_2]_4$, clearly confirm the unusual selectivity of these bidentate dendritic ligands and show that a 'positive dendritic effect' occurs. This high selectivity is obtained with only one structure within the 1st and 2nd generation dendrimer (spacer of five atoms between the phosphorus atoms, and carbon–silicon linkage) whilst other frameworks (spacer of three and seven atoms between the P atoms, or carbon–oxygen–silicon linkage) lead to lower selectivity.

Introduction

The hydroformylation of long chain alkenes to form aldehydes is an important industrial process.[1] However, the use of rhodium complexes, which show high reactivity and selectivity, is restrained by the cost and difficult recovery of such transition metals. To our knowledge, no efficient recovery process has yet been successfully applied on an industrial scale for long chain alkenes, although a pilot plant is currently under construction for a process using low pressure distillation of the product. The use of dendrimers could help to overcome this problem since their size allows recycling of the catalyst using ultra filtration techniques.[2,3] Several examples of such catalyst recovery have recently been reported.[4–6] Because two major products are formed during the hydroformylation reaction (linear and branched aldehydes), the design of a ligand favouring mainly the linear aldehyde is desirable. High regioselectivity is found when using large excesses of *e.g.* PPh_3 [1] or with bidentate phosphine chelates such as bis(diphenylphosphino)methyl biphenyl (BISBI)[7] and Xantphos[8] type ligands, which give the highest regioselectivities (ratio > 50 : 1 to the linear aldehyde).

There are now a number of examples of the use of dendrimers as catalytic ligands in the literature. However, they show varying degrees of effect on the processes, with only a few showing properties that are different from those of small molecule analogues. These range from total inhibition of the reaction[9] to an improvement in reactivity.[4,10–12] Shape-selective catalytic reactions have also been reported.[13,14] However, to our knowledge, improved product selectivity using these macromolecule ligands has only been reported by Fan *et al.* for hydrogenation reactions using a BINAP type ligand,[15] by Mizugaki *et al.* for the stereoselective allylic amination[16] and by ourselves for the hydroformylation of linear alkenes.[17–20] Other dendrimer systems used in hydroformylation reactions did not show such a property.[21–25] We report here that 1st and 2nd generation polyhedral oligomeric silsesquioxane (POSS) dendrimers containing diphenylphosphine moieties at their periphery are successful as ligands for rhodium in the hydroformylation of oct-1-ene. Unexpectedly high regioselectivity to the linear aldehyde (l : b = 14 : 1) was found for a specific type of POSS dendritic ligand, *i.e.* 1st and 2nd generation dendrimers (respectively with 16 or 48 diphenylphosphine end groups) with a spacer of five atoms between the P atoms, whilst the small molecule analogues and the other dendritic ligands prepared (different arm length or composition) showed lower selectivity. Dendrimers in this paper are described by their generation number, G1 = 1st generation, G2 = 2nd generation *etc*. and the type and number of terminal functionality, *e.g.* G1-16vinyl is a 1st generation dendrimer terminated by 16 vinyl groups. Preliminary communications of some of this work have appeared.[18–20]

Results and discussion

Synthesis

The phosphine containing dendrimers were derived from the G1-16Cl, G1-24Cl and G1-16vinyl, G1-24vinyl, G2-propyl-48vinyl dendrimers[17,26] by nucleophilic substitution of the chlorine atoms of the terminal chlorosilane groups, or by radical addition reactions of secondary phosphines onto the vinyl end groups. Using these two methods, we have synthesized a series of phosphine-based dendrimers with terminal PR_2 groups (R = C_6H_5, $C_6H_3(CF_3)_2$) (Table 1). The phosphorus atoms were separated on the same arm by a spacer of three, five or seven atoms, the central one of which was a silicon atom. The interest in varying the dendritic structure arose from preliminary results obtained by van Leeuwen[23] and our group[18–20] showing different selectivity for different arm lengths. The compounds were characterized by NMR, MALDI-TOF (Matrix Assisted Laser Desorption Ionization-Time of Flight) mass spectrometry and microanalysis.

† Electronic supplementary information (ESI) available: plots showing the effect of temperature and dendrimer structure on the rate of hydroformylation of oct-1-ene. See http://www.rsc.org/suppdata/dt/b2/b206597e/

DOI: 10.1039/b206597e

Table 1 Diphenylphosphine functionalised POSS dendrimers

Entry	Dendrimer	Synthetic method	^{31}P NMR δ/ppm	Conversion[a] (%)	Yield[a] (%)
1	G1-16ethylPPh$_2$	1[b]	−9.6, −9.7, −14.4 (w)	>99[f,g,h]	95
2	G2-propyl-48ethylPPh$_2$	1[b]	−9.9 (br)	84[f]	77
3	G1-24ethylPPh$_2$	1[b]	−9.5 (br)	60[f,g]	95
4	G1-16propylPPh$_2$	1[b]	−17.3	56[f]	96
5	G1-16ethylPAr$_2$ Ar = 3,5-C$_6$H$_3$(CF$_3$)$_2$	1[b]	−6.6, −6.9, −7.0, −12.9	75[f]	92
6	G1-24methylPPh$_2$	2[c]	−23.9	60[f,g]	93
7	G1-16methylPPh$_2$	2[c]	−22.6 (br), −22.7 (w)	>95[f,g]	60–70
8	G1-16methoxyPPh$_2$	3[d]	−13.6 (br)	>86[f,g]	76
9	G1-16ethoxyPPh$_2$	3[d]	−22.3, −22.5	>92[f,g]	85
10	G1-16propylPPh$_2$	4[e]	−16.1, −16.2, −16.3 (w), −16.4	>85[f]	75

[a] Yield refers to the isolated chemical yield; conversion refers to the percentage of vinyl or chloro groups converted to phosphines. [b] Addition of HPPh$_2$ to vinyl or allyl POSS. [c] Reaction of R$_2$PCH$_2$Li with chlorosilane derivatised dendrimer. [d] Reaction of Ph$_2$P(CH$_2$)$_n$OH with –SiMeCl$_2$ derivatised G1 dendrimer. [e] Reaction of Ph$_2$P(CH$_2$)$_3$MgBr with –SiMeCl$_2$ derivatised G1 dendrimer. [f] ^{1}H NMR. [g] MALDI-TOF. [h] Microanalysis.

Following the same experimental method as previously described for diethylphosphine type dendrimers,[17] the reaction of diphenylphosphine (excess) with the vinyl substituted POSS was carried out using AIBN as a radical initiator to give the corresponding diphosphine-functionalised POSS. Quantitative yield and excellent to good conversions were obtained for G-16ethylPPh$_2$ (complete conversion) and G2-propyl-48ethylPPh$_2$ (84% conversion) (Table 1, Entries 1 and 2).

However, only 60% conversion was reached for the 24 arm counterpart, G1-24ethylPPh$_2$ (Table 1, Entry 3), probably due to steric crowding. For this reason, this dendrimer has only been characterised by NMR spectroscopy. The ^{31}P NMR spectra showed that the phosphine groups in the same dendrimer for the three compounds were not all equivalent. Indeed two major and one minor peak were found for the 16-branched dendrimer G1-16ethylPPh$_2$ (Table 1, Entry 1) at δ −9.6, −9.7 ppm (major) and δ −14.4 ppm (minor). Broad signals centered at δ −9.9 ppm for G2-propyl-48ethylPPh$_2$ (Table 1, Entry 2) and at −9.5 ppm for G1-24ethylPPh$_2$ (Table 1, Entry 3) were detected. We assume that several P environments are observed for these dendrimers mainly because the conversion is not complete. This means that some arms will have 3, 2 or 1 -PPh$_2$ termini. These may well have different ^{31}P NMR spectral resonances. In addition, back-folding of a phosphine terminus inside the dendrimer could lead to a different ^{31}P NMR shift. The excess of phosphine was removed at 120 °C under vacuum or by silica gel column chromatography. Although lower yields were obtained using chromatography (86%), no change in the conversion of the product was found. These compounds were low melting point air sensitive solids, which were extremely soluble in most organic solvents, except polar ones such as ethanol. ^{1}H NMR spectra and the microanalysis did not show the presence of unreacted vinyl groups in G1-16ethylPPh$_2$ but further characterization by MALDI-TOF MS showed the presence of mainly 14, 15 or 16 phosphine groups. This suggests that fragmentation occurred during the MALDI-TOF analysis. In addition, the compound was found to be partially oxidized (which probably occurred during the MS analysis process) since mass increments of 16 due to the oxygen atoms were present in the spectrum.

Addition of HPPh$_2$ to the allyl POSS G1-16allyl[17] to prepare the propyl analogue G1-16propylPPh$_2$ failed since even after heating for two weeks and several additions of radical initiator only 56% conversion was obtained (Table 1, Entry 4). This poor conversion is probably due to the lesser reactivity of the allyl silane.

Attempts to introduce arylphosphines with electron withdrawing groups (radical addition of bis[3,5-(trifluoromethyl)-phenyl]phosphine[27]) into the periphery of the dendrimer were also carried out. Such compounds are very interesting as ligands since the electron withdrawing groups may improve the selectivity of the hydroformylation reaction, although this depends on the configuration of the complex.[27–29] The complete radical addition of the fluorinated arylphosphine onto the G1-16vinyl[17] compound failed since 25% of unreacted vinyl groups were still present after one month, even after numerous consecutive additions of AIBN. The substituted POSS compound (G1-16ethylPAr$_2$, Ar = 3,5-C$_6$H$_3$(CF$_3$)$_2$) showed four ^{31}P signals at δ −6.6, −6.9, −7.0 and −12.9 ppm, indicating a variety of phosphorus environments in such a partially substituted compound (Table 1, Entry 5). As expected these ^{31}P NMR resonances are shifted to higher frequency by an average of 2–3 ppm compared with the diphenylphosphine substituted analogue.

Substitution of the chlorine atoms of the chlorosilane POSS by nucleophiles allows us to modify the internal structure of our diphenylphosphine containing dendrimer. Addition of LiCH$_2$P(C$_6$H$_5$)$_2$-TMEDA[30] in excess to G1-24Cl[26] failed to give satisfactory results since after 3–5 days of reaction, only partial substitution (60%) was reached (Table 1, Entry 6). It is believed that this was caused by the steric hindrance of the diphenylphosphine groups. As the complete substitution of the 24-Cl POSS failed, we prepared the homologue with 16 arms G1-16methylPPh$_2$. Good conversion was obtained (>95%, Table 1, Entry 7). A major peak was found in the MALDI-TOF spectrum at m/z = 4176 (M$^+$ = 4173.5). Interestingly, fragmentation clearly occurred since a peak at m/z [M − (PPh$_2$)] was identified in the mass spectrum. Good purity products were obtained by silica gel column chromatography with 60–70% yields of a white solid. The ^{31}P NMR spectrum showed two resonances at δ −22.6 and −22.7 ppm. Shorter reaction times led to the formation of partially substituted products with *e.g.* 12–13 arms.

Diphenylphosphino alcohol compounds were also used to introduce phosphine moieties into the dendrimer. Addition of these alcohols to G1-16Cl[17] in the presence of base led to diphenylphosphine-containing dendrimers with different length spacers between the phosphorus atoms. Diphenylphosphinomethanol (prepared *in situ*)[31] was added in excess (3 to 1) to the 16-chloro POSS in the presence of triethylamine. Good conversion (>86%, Table 1, Entry 8) to the G1-16methoxyPPh$_2$ compound was obtained after six days (only 60% after two days). After purification through silica gel column chromatography, a colourless non-crystalline product was isolated in 76% yield. ^{1}H NMR and MALDI-TOF MS showed that an average of 14 arms (of the possible 16) contained the diphenylphosphine species (conversion >86%). Partial fragmentation may also have occurred since peaks at m/z {M − x(CH$_2$PPh$_2$)} were found (x = 0, 1, 2, 3, *etc.*). A single signal in the ^{31}P NMR was found at δ −13.6 ppm confirming the presence of the phosphine species.

To vary the chain length between the phosphorus atoms, excess 2-diphenylphosphinoethanol[32] was reacted with G1-16Cl. The product, G1-16ethoxyPPh$_2$, was purified by silica gel

Table 2 Results of hydroformylation reactions of oct-1-ene using G1-16ethylPPh$_2$ ligands

Entry	Ligand	T/°C	P/bar	t/h	k/10^{-3} s^{-1}	Conversion (%)	Isomerisation (%)	l : b ratio	Nonan-1-al (%)
1	A[b]	80	20	24	0.05	>99.9	2.5	6.6	83.9
2	A[b]	80	10	19	0.08	> 99.9	6.0	8.8	83.5
3	A[b]	100	10	4	0.42	> 99.9	5.0	10.8	86.2
4	A[b]	120	10	2	1.1	> 99.9	6.3	12.0	85.6
5	A[b]	100	20	6	0.33	> 99.9	3.2	7.5	84.7
6	B[a]	120	10	2	1.2	> 99.9	6.6	13.9	86.0
7	A[b]	120	10	0.2	1.1	56.7	6.6, 14[c]	15.4	48.5, 86[c]

Reaction conditions: [Rh(acac)(CO)$_2$] (2.0 × 10^{-5} mol), toluene (4 cm^3), oct-1-ene (8.3 × 10^{-3} mol), CO : H$_2$ = 1 : 1.[a] G1-16ethylPPh$_2$ dendrimer with 16 arms functionalised, P : Rh = 6 : 1. [b] G1-16ethylPPh$_2$ dendrimer with 12 arms functionalised P : Rh = 5.4 : 1. [c] Based on the amount of oct-1-ene consumed.

column chromatography to give a non-crystalline solid in 85% yield (Table 1, Entry 9). An average of 14–15 arms were converted to the phosphine species (>92%). The MALDI-TOF spectrum showed a large distribution of peaks. However, partial decomposition occurred during the MALDI-TOF analysis since the observed peaks correspond to {M − x(CH$_2$-CH$_2$PPh$_2$)} (x = 0, 1, 2, 3, *etc.*) rather than {M − x[(OCH$_2$-CH$_2$PPh$_2$) + Cl]} or more probably at {M − x[(OCH$_2$-CH$_2$PPh$_2$) + OH], which would be expected if only partial substitution had occurred. The ^{31}P NMR spectrum showed two broad signals centered at δ −22.3 and −22.5 ppm indicating that not all the phosphorus atoms were in identical environments. To obtain a more stable compound (than the one with a siloxane linker) with a seven atom spacer between the two phosphorus atoms, we reacted the Grignard species ClMg(CH$_2$)$_3$PPh$_2$ [33] with the 16-chloro POSS. The addition of an excess (three fold) of the Grignard compound to G1-16Cl POSS afforded a partially functionalized POSS G1-16propylPPh$_2$ (76% conversion after 36 h, Table 1, Entry 10). After four days only a slight increase of the conversion was obtained since 86% (^{1}H NMR) of the chlorides were substituted. The compound was then isolated after work up as a colourless non-crystalline solid in 75% yield. Four ^{31}P chemical shifts were found at δ −16.1, −16.2, −16.3 and −16.4 ppm indicating the different environments of the phosphorus atoms. The microanalytical data and the MALDI-TOF mass spectrum of this complex were not in agreement with the proposed formula, so the assignment of the structure of this dendrimer must be regarded as only tentative.

In summary, we have synthesized POSS centred dendrimer bound alkyldiphenylphosphines with at least two phosphine groups per dendrimer branch. The P atoms are separated by three, five or seven atoms. The central atom is always Si and the other atoms may be all C or two of them may be O. When O is present, it is always adjacent to the Si atom. Generally speaking the Si atom is attached to the POSS core by a two carbon spacer, although three carbon spacers are used in G2-propyl-48ethylPPh$_2$.

Catalytic reactions

Hydroformylation using rhodium complexes of G1-16ethylPPh$_2$ and small molecule analogues. G1-16ethylPPh$_2$ was reacted *in situ* with [Rh(acac)(CO)$_2$] and the resulting solutions used for the hydroformylation of oct-1-ene. With Rh : P > 3 : 1, the catalytic complexation occurred in a few seconds to give homogeneous yellow or orange solutions depending on the concentration of rhodium and/or dendrimer. Under H$_2$/CO pressure these solutions turned bright yellow and they had a similar appearance after the hydroformylation reactions. Low phosphine : rhodium ratios (≤3 : 1) led to the formation of an insoluble solid (*via* a gel). Attempts to re-dissolve the precipitate failed. This is possibly due to cross-linking of the dendrimers through rhodium, as the P : Rh ratio in the system decreases, leading to oligomeric dendrimer species. Although bidentate coordination might be expected, the many different phosphorus environments may mean that when a larger amount of rhodium is loaded, all of the bidentate sites are filled and some rhodium binds between two single P atoms on different dendrimers.

The catalytic reactions were carried out using different batches of G1-16ethylPPh$_2$ ligand since a first synthesis led to incomplete conversion to the desired dendrimer (12 arms substituted out of 16). This partially functionalized ligand will be named 'A'. The second type of dendritic ligands used (different batches) was shown to have more than 15 arms functionalized (ligand named 'B'). A first set of experiments was carried out using ligand A at 80 °C under 20 bar of H$_2$/CO with a phosphine : rhodium ratio of 5.4 : 1. After reaction (<24 h, Table 2, Entry 1) high conversion to the aldehydes, nonan-1-al and 2-methyloctan-1-al was observed. High selectivity to the linear aldehyde (83.9%) with a linear to branched ratio (l : b) of 6.6 : 1 was obtained. A first order dependence in substrate and rhodium was determined for this reaction. Similar results although with a slightly increased rate were obtained at lower CO/H$_2$ pressure (Table 2, Entry 2).

Higher temperatures, *i.e.* 100 and 120 °C (H$_2$/CO 10 bar), increased the reaction rate allowing completion of the reaction respectively in four and two hours (Table 2, Entries 3 and 4). These higher reaction temperatures combined with lower CO/H$_2$ pressure (10 bar) led also to an increased selectivity to the linear aldehyde (up to 85.6%) with an improved l : b ratio of 10.8 or 12 : 1 (*cf.* 7.5 at 20 bar and 100 °C, Table 2, Entry 5). The gas uptake plots at different temperatures showing the first order kinetics are shown in the ESI, Fig. S1. Even higher selectivity was obtained under these conditions (120 °C, 10 bar) with the more crowded dendrimer B (Table 2, Entry 6), since 86.0% of the product was nonan-1-al with a l : b ratio of 13.9 : 1. It thus appears that, for a given P : Rh ratio (5.4 : 1), both the rate constant (from 0.08 × 10^{-3} to 1.1 × 10^{-3} s^{-1}) and l : b ratio (from 6.6 to 12) markedly increased when the pressure was lowered (compare entries 1 and 2 or 5 and 3 in Table 2) or the temperature increased (compare entries 2, 3, and 4 in Table 2). This increased selectivity is probably related to β-H-elimination, since isomerisation is more prevalent when the l : b ratio is higher.[1,32] In all cases, traces of hydrogenated product, nonan-1-ol (<0.4%), and substrate, octane (0.5–1.4%), were detected, but the major side products were isomerised octenes (Table 2).

The intrinsic l : b ratio (15.4 : 1) for the hydroformylation of oct-1-ene by rhodium complexes of G1-16ethylPPh$_2$ was obtained by running the hydroformylation over a short period (0.2 h). Longer reaction times led to less selective reactions, probably because some of the isomerised alkenes are converted into branched aldehydes (Table 2, Entry 7).

The effect of the phosphine : rhodium ratio under fixed reaction conditions (10 bar of H$_2$/CO, 120 °C, [Rh] = 3.77 × 10^{-3} mol dm^{-3}) was also studied. It was found that the dendrimer could only support a limited amount of rhodium species since when a P : Rh ratio of 2 : 1 was used, precipitation of a metallic residue occurred with a lowering of the rate

Table 3 Results of hydroformylation reactions of oct-1-ene varying the phosphine/rhodium ratios using G1-16ethylPPh$_2$ ligands[a]

Entry	Ligand	P : Rh	$k/10^{-3}$ s^{-1}	Isomerisation (%)	l : b ratio	Nonan-1-al (%)
8	B	2	0.52	35.5	3.4	48.4
9	A	3.6	0.95	7.1	11.9	84.3
10	A	5.4	1.1	6.3	12	85.6
11	A	10.8	1.5	6.6	12.2	85.2

[a] [Rh(acac)(CO)$_2$] (2.0×10^{-5} mol), P : Rh = 6 : 1, toluene (4 cm^3), oct-1-ene (8.3×10^{-3} mol), 120 °C, CO/H$_2$ 10 bar, total reaction time 2 h, conversions all >99.9%.

Table 4 Comparative study on the hydroformylation reaction of oct-1-ene using small molecule analogues of the dendrimer-based ligands

Ligand	$k/10^{-3}$ s^{-1}	Oct-2-ene (%)	3- + 4-Octene (%)	Nonan-1-al (%)	l : b ratio
1	3.6	10.6	0.83	70.1	3.4
2	3.0	5.8	0.90	72.7	3.8
3	2.1	6.2	0.40	77.4	5.2

Reaction conditions: [Rh(acac)(CO)$_2$] (2.0×10^{-5} mol), P : Rh = 6 : 1, toluene (4 cm^3), oct-1-ene (8.3×10^{-3} mol), 120 °C, CO/H$_2$ 10 bar, total reaction time 2 h, conversion all > 99.5%.

constant and aldehyde l : b ratio (3.4 : 1) (Table 3, Entry 1). This may be related to the formation of oligomeric complexes, as discussed above, although the large amount of isomerised alkene may indicate that significant amounts of unligated rhodium, which could also be responsible for the rhodium plating, are also present. Interestingly, increasing the P : Rh ratio from 3.6 to 10.8 : 1 (ligand A) led to a higher rate constant (Table 3, Entries 9–11) while the l : b ratio stayed virtually unchanged at *ca.* 12—the upper limit that we have observed for dendrimer A. A possible explanation for this unusual behaviour is that rhodium is strongly bound to the dendrimer, probably *via* two P atoms, and that steric constraints prevent the coordination of extra P atoms to block vacant sites and inhibit the reaction, as is observed when using triphenylphosphine.

The high selectivity to nonan-1-al observed with these dendrimer-based ligands was surprising since potentially bidentate ligands with a spacer of five atoms (or more) between the two P atoms usually only show high linear selectivity if the backbone is constrained in some way, as for BISBI[7] and Xantphos[8] type ligands, although certain flexible analogues of Xantphos containing P(CH$_2$)$_2$O(CH$_2$)$_2$P backbones can give l : b ratios up to 9.2.[34]

In order to determine the exact influence of the dendrimer structure on the reactivity and selectivity of the catalytic reaction, the hydroformylation of oct-1-ene was carried out using small molecules as ligands with structures related to those of the dendrimer based phosphines. 1,5-Bis(diphenylphosphino)pentane (**1**), bis(diphenylphosphinoethyl)dimethylsilane (**2**), and tetrakis(diphenylphosphinoethyl)silane[35] (**3**) (Fig. 1) were used for the *in situ* formation of rhodium complexes and

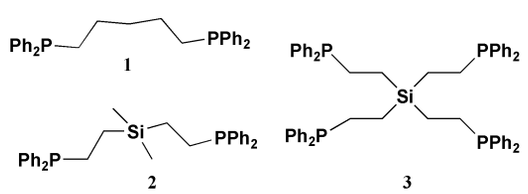

Fig. 1 Small molecule analogues of the dendrimers used as ligands in the hydroformylation reaction.

their use in catalysis under the conditions of Table 2, Entry 1. The results of the reactions are reported in Table 4 and Fig. 2. Whilst the dendrimer gave a selectivity to the linear aldehyde, nonan-1-al, of 86%, the small molecules **1**, **2** and **3** respectively led to 70.1, 72.7, and 77.4% selectivity to the desired aldehyde (Table 4) clearly showing that there is a positive dendritic effect on the selectivity of the reaction. Selectivities obtained using the small molecules and the dendrimer-based ligands are shown in Fig. 2. The rates of reaction using the small molecules were, however, higher than those found when using the dendrimer-based ligand.

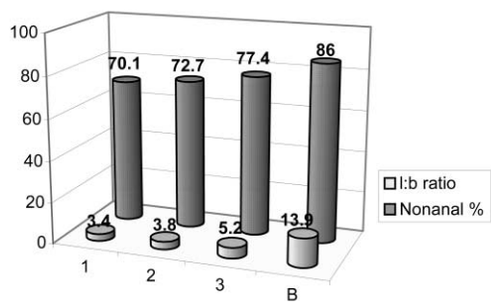

Fig. 2 Selectivity to nonan-1-al and l : b ratio in hydroformylation reactions of oct-1-ene using G1-16ethylPPh$_2$ POSS, B or small molecule analogues. **1** = H$_2$C(CH$_2$CH$_2$PPh$_2$)$_2$, **2** = Me$_2$Si(CH$_2$CH$_2$PPh$_2$)$_2$, **3** = Si(CH$_2$CH$_2$PPh$_2$)$_4$.

The selectivity using **3**, which can be thought of as a first generation dendrimer, albeit with a different core was better than that obtained with **2**. **2** was also found to give a higher selectivity than the less hindered ligand, **1**. As expected for the more sterically crowded phosphine ligand **3**, the rate constant, which was 3.0×10^{-3} s^{-1} for **2**, dropped to 2.1×10^{-3} s^{-1} (P : Rh = 6 : 1).

Using **3** the selectivity to nonan-1-al rose from 55.9 to 79.9% when phosphine : rhodium ratios of respectively 2 : 1 to 12 : 1 were used. This type of dependence is reminiscent of that obtained when using unidentate rather than bidentate phosphines. No such effect was found for the dendrimer-based ligand, confirming the strong chelation of the dendrimer to rhodium.

Hydroformylation using rhodium complexes of G1-24methylPPh$_2$. In order to examine the effect of the spacer length between phosphine groups in the dendrimer upon the hydroformylation reactions, catalytic solutions prepared *in situ* from G1-24methylPPh$_2$ (incomplete substitution, *i.e.* 60% functionalised and [Rh(acac)(CO)$_2$] or [Rh$_2$(O$_2$CMe)$_4$] was used for the hydroformylation of hex-1-ene under various different conditions. The l : b ratio was never higher than 2.3 at a P : Rh ratio of 4 : 1 (Table 5, Entry 12) and dropped slightly as the amount of dendrimer added was reduced (Table 5, Entries 12–15). Similar results were obtained at lower rhodium concentration (Table 5, Entry 16) or replacing toluene with ethanol (Table 5, Entry 17), although in this last reaction, small amounts of alcohol

Table 5 Hydroformylation of hex-1-ene catalysed by rhodium complexes formed with the G1-24methylPPh$_2$ dendritic ligand

Entry	Solvent	[Rh]/10^{-3} mol dm^{-3}	P : Rh	*t*/h	Conversion (%)	Aldehydes (%)	Alcohols (%)	l : b ratio[a]
12	Toluene	8	4	2.5	95	92	—	2.3
13	Toluene	8	3	2.5	95	92	—	2.3
14	Toluene	8	2	4	>99	96	—	2.0
15	Toluene	8	1.5	4	>99	97	—	1.9
16	Toluene	4	3	2.5	89	86	—	2.4
17	Ethanol	8	4	16	>99	93	5	1.8

Reaction conditions: [Rh$_2$(O$_2$CMe)$_4$] or [Rh(acac)(CO)$_2$] (entry 12 only), solvent 4 cm^3, hex-1-ene 8.0 × 10^{-3} mol, 120 °C, H$_2$/CO 40 bar.[a] Linear to branched ratio of aldehyde only.

Table 6 Hydroformylation of oct-1-ene catalysed by Rh complexes of POSS derived dendrimer diarylphosphines

Entry	Ligand	*t*/h	Rate/10^{-3} s^{-1}	Isomer (%)	Nonan-1-al (%)	l : b ratio
18	G1-16methylPPh$_2$	0.3	6.2	12.1	68.5	3.9
19	G1-16ethylPAr$_2$[a]	2	1.1	20.0	73.0	15.0
20	G1-16methoxyPPh$_2$	2	0.7	9.0	76.2	5.7
21	G1-16propylPPh$_2$	2	1.5	5.1	78.0	5.0
22	G1-16ethoxyPPh$_2$	2	2.0	8.3	78.1	6.4
23	G2-propyl-48ethylPPh$_2$	3	0.6	7.5	83.8	11.5

Reaction conditions: [Rh(acac)(CO)$_2$] = 2.0 × 10^{-5} mol, P : Rh = 6 : 1, substrate 8.3 × 10^{-3} mol, toluene (4 cm^3), 120 °C, CO/H$_2$ 10 bar, conversion all >99.9%.[a] Ar = 3,5-C$_6$H$_3$(CF$_3$)$_2$.

were formed. The best selectivity obtained to the linear aldehyde, heptan-1-al, was 67.5% with a linear to branched ratio of 2.3 : 1 (Table 5, Entries 12 and 13).

Interestingly, extensive studies carried out by van Leeuwen and co-workers showed that a compound derived from tetravinylsilane containing 16 Ph$_2$P arms, but with only one CH$_2$ spacer between the silicon and phosphorus atoms (*i.e.* the same end groups as in G1-24methylPPh$_2$) also gave an l : b ratio of 2.3 : 1, the same as that obtained using the small molecule analogue (Me$_2$Si(CH$_2$PPh$_2$)$_2$).[23] Thus, the spacer length between the P atoms seems to be important in determining whether or not an enhanced linear selectivity is obtained when using dendrimers based on phosphines as ligands for rhodium catalysed hydroformylation reactions.

Hydroformylation using rhodium complexes of other dendrimers nominally with 16 PPh$_2$ end groups; varying the spacer length and the atoms in the spacer group. Since the regioselectivity of the reaction was different using the dendritic ligand, G1-24methylPPh$_2$ from that obtained with G1-16ethylPPh$_2$, it was interesting to compare the latter ligand with other 16-branched dendrimers. The reactions were carried out under the optimal conditions found for G1-16ethylPPh$_2$ and the results are summarised in Fig. 3 and Table 6.

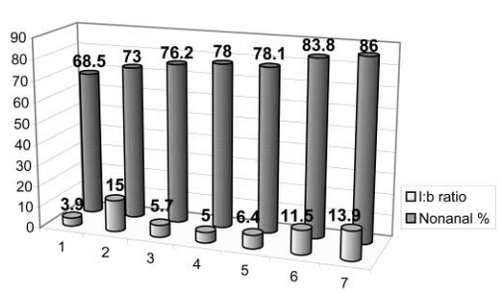

Fig. 3 Selectivity to nonan-1-al and l : b ratio using different POSS dendritic ligands, 1 = G1-16methylPPh$_2$, 2 = G1-16ethylPAr$_2$, 3 = G1-16methoxyPPh$_2$, 4 = G1-16propylPPh$_2$, 5 = G1-16ethoxyPPh$_2$, 6 = G2-propyl-48ethylPPh$_2$, 7 = G1-16ethylPPh$_2$ (dendrimer B).

The G1-16methylPPh$_2$ dendritic ligand gave similar results in the hydroformylation of oct-1-ene (68.5% nonan-1-al, Entry 18, Table 6) to those of its counterpart G1-24methylPPh$_2$ for hex-1-ene (67.5% heptanal, Entry 12, Table 5, although at 40 bar). These selectivities are considerably lower than those obtained with G1-16ethylPPh$_2$, confirming that a three atom spacer between P atoms does not afford enhanced linear selectivity. The rate of reaction with this G1-16methylPPh$_2$ is *ca.* six times higher than for the G1-16ethylPPh$_2$ dendritic ligand (Table 2, Entry 6). In addition, a high amount of isomerised substrate (12.2%) is formed with the shorter spacer. Modelling studies, to be reported separately,[36] show that the three atom spacer does not place the P atoms in the optimal relative position for bidentate coordination with both P atoms in equatorial positions in five-coordinate intermediates.

The hydroformylation of oct-1-ene using the dendritic ligand G1-16ethylPAr$_2$ (Ar = 3,5-C$_6$H$_3$(CF$_3$)$_2$) was also carried out under similar reaction conditions. Interestingly, the pre-formed catalytic mixture (in toluene) was heterogeneous at room temperature showing an extremely pale brown solution and a brown oily residue. This heterogeneity is remarkable since both the rhodium-based catalyst, [Rh(acac)(CO)$_2$], and the dendrimer were independently soluble in toluene. A homogeneous orange–brown solution was however obtained in warm toluene. The hydroformylation of oct-1-ene catalyzed by this dendritic rhodium complex gave 73.0% selectivity to nonan-1-al (Table 6, Entry 19), however the reaction gave a high l : b ratio (15 : 1). This ligand promotes significant isomerisation activity (20%), but is inactive for the hydroformylation of internal alkenes; only traces of 2-ethylheptan-1-al were formed.

Surprisingly the dendritic ligand G1-16methoxyPPh$_2$, which has a similar structure that of G1-16ethylPPh$_2$ (the methylene group attached to the peripheral Si atom is replaced by O), and so should form similar rhodium complexes, did not lead to high selectivity to nonan-1-al. Indeed, whilst 86.0% of the product was the linear aldehyde using G1-16ethylPPh$_2$ (Table 2, Entry 6) only 76.2% of nonan-1-al was formed using the rhodium/G1-16methoxyPPh$_2$ species (Table 6, Entry 20). Therefore not only is the length of the bridge between the P atoms an important factor in determining the selectivity of the reaction, but also the composition of this bridge can influence the selectivity of the catalytic species. It is important to note that the electronic properties of the phosphine species on the two different dendrimers differed since ^{31}P NMR resonances were at δ_P −9.4 and −13.6 ppm for G1-16ethylPPh$_2$ and G1-16methoxyPPh$_2$, respectively. It should also be noted that a small amount of precipitate (yellow solid) was found at the end of the reaction using G1-16methoxyPPh$_2$ indicating that the dendritic ligand

may not be completely stable under the reaction conditions (the pre-formed catalytic solution was bright yellow with no precipitate and it is not known whether the precipitate occurred during the reaction or after cooling and depressurisation). However, since the kinetics of the hydroformylation reaction were first order in oct-1-ene, it is unlikely that the differences observed in the distribution of the products arose from decomposition of the catalyst. Another explanation considered is that there may be a different geometry of the two dendrimers due to the oxygen atom linker. Indeed if such a difference exists, as suggested by very preliminary modelling studies on this dendrimer which suggest that it is more compact than the G1-16ethylPPh$_2$, it would modify the mode of coordination of the phosphine species in the rhodium complexes, possibly leading to different catalytic species and so different reactivity and selectivity. The lower rate of reaction obtained with this ligand (compared to the G1-16ethylPPh$_2$ system) supports such a hypothesis. Isomerisation of the substrate was relatively high since 8.82 and 0.22% of the products were respectively oct-2-ene and oct-3-ene. This high isomerisation rate led to a relative good l : b ratio of 5.7 : 1. The isomerisation is not followed by hydroformylation of the internal alkenes since only traces of 2-ethylheptanal were found (0.17%).

The use of the dendritic ligands G1-16propylPPh$_2$ (Table 6, Entry 21) and G1-16ethoxyPPh$_2$ (Table 6, Entry 22) further emphasises the importance of the spacer length for obtaining high linear selectivities using this type of dendrimer-based ligand. Indeed the regioselectivity to the linear aldehyde during the hydroformylation of oct-1-ene was lower with these two ligands (*ca.* 78% for both) than with the G1-16ethylPPh$_2$ dendritic ligand (86%) (Table 2, Entry 6). Nevertheless, these selectivities are still higher than those obtained with small molecules (Table 4). Interestingly, unlike for G1-16ethylPPh$_2$ and G1-16methoxyPPh$_2$, the different electron density of the phosphorus atoms of these two dendrimers, G1-16ethoxyPPh$_2$ and G1-16propylPPh$_2$, did not seem to influence the selectivity of the reaction. Indeed although different ^{31}P NMR chemical shifts were found respectively at δ_P −22.5 and −16.5 ppm for G1-16ethoxyPPh$_2$ and G1-16propylPPh$_2$, the selectivities to nonan-1-al were 78.1 and 78.0% (Table 6, Entries 21 and 22). G1-16ethoxyPPh$_2$ led to a higher linear to branched ratio than G1-16propylPPh$_2$ (l : b = 6.4 : 1 compared to 5.0 : 1), due to the presence of larger amounts of isomerised alkenes (2-, 3- and 4-octene: 8.3% for G1-16ethoxyPPh$_2$, 5.1% for G1-16propylPPh$_2$) in the final product solution. Also a slightly higher rate was observed for G1-16ethoxyPPh$_2$ (2.0×10^{-3} instead of 1.5×10^{-3} s^{-1}). Nevertheless the rates of reaction using these two ligands were higher than those obtained using the more selective G1-16ethylPPh$_2$ dendrimer, data which are consistent with a weaker phosphine to rhodium interaction and so lower regioselectivity. It is thus believed that these dendrimers do not constrain the phosphine end groups to optimum coordination to rhodium due to the longer chain length (spacer of seven atoms). BISBI and Xantphos do have longer spacer lengths, but here the backbone is heavily constrained.

Using the second generation dendritic ligand with the optimum –(CH$_2$)$_2$Si(CH$_2$)$_2$– spacer between the P atoms, G2-propyl-48ethylPPh$_2$ (only functionalised to 85%) rather similar results in terms of selectivity were obtained to those using the G1-16ethylPPh$_2$ dendritic ligand. Indeed, using G2-propyl-48ethylPPh$_2$ as ligand (Table 6, Entry 23), the regioselectivity to the linear aldehyde, nonan-1-al, was 83.8% with a l : b ratio of 11.5 : 1 whilst the 16 arm ligand gave a selectivity of 86.0% and a l : b ratio of 13.9 : 1 (Table 2, Entry 6). A drop in the rate of reaction by a factor *ca.* 2 was nevertheless apparent (Table 6, Entry 23), perhaps because the steric hindrance of such bulky ligands reduced the accessibility of the rhodium centre. Steric bulk might also explain the slight increase in isomerisation products for the larger dendrimer-based ligand (7.5 instead of 6.6% with G1-16ethylPPh$_2$, **B**), since it was also found that the isomerisation process increased marginally when passing from the partially functionalised G1-16ethylPPh$_2$ **A** to the bulkier G1-16ethylPPh$_2$ **B** (Table 2, Entries 4 and 6).

Reactions with all the dendritic complexes showed a first order dependence on substrate concentration (see Fig. S2, ESI). The perfect straight lines of the plots of ln{[$P(t)$ − P(min)]/[P(0) − P(min)]} *versus* time of the different dendrimers clearly confirm that only hydroformylation of oct-1-ene occurred without other side reactions consuming H$_2$ or CO. The least regioselective and most compact ligand, G1-16methylPPh$_2$, led to the highest rate of reaction (*ca.* three times the rate found with G1-16ethylPPh$_2$) while the less sterically hindered ligands G1-16ethoxyPPh$_2$ and G1-16propylPPh$_2$, showing intermediate selectivity, led to rate constants slightly higher than the G1-16ethyl PPh$_2$ catalytic system (Fig. S2, ESI). However, the correlation between selectivity and rate of reaction, *i.e.* high selectivity coupled with low rate, is not straightforward. Indeed, although G1-16methoxyPPh$_2$ led to the lowest rate of reaction for the 1st generation dendrimers ($k = 0.7 \times 10^{-3}$ s^{-1}), a low regioselectivity to nonan-1-al was obtained (76.2%). The rate constant using the second generation dendrimer, G2-propyl-48ethylPPh$_2$, was *ca.* half that for the G1-16ethylPPh$_2$ system whilst G1-16ethylPAr$_2$ gave similar kinetics to those of its unfluorinated counterpart.

Characterization of catalysts

High pressure ^{31}P NMR studies. The generally high l : b ratios obtained using G1-16ethylPPh$_2$ suggest that strong bidendate coordination occurred [1] or that the high local concentration of phosphorus atoms on the surface of the dendrimer increased the concentration of complexes containing three P donors.[37–39] The mechanism of reaction for these two hypotheses would therefore be similar to the one proposed by Wilkinson and co-workers.[37,38] Another possibility for such selectivity could be the formation of bimetallic species as reported by Stanley and co-workers.[40,41] We have attempted to obtain information on the species present in solution by using ^{31}P NMR spectroscopy, molecular mechanics simulations and HP IR spectroscopy.

As discussed previously the dendritic species G1-16ethylPPh$_2$ seems to chelate strongly to the rhodium since the selectivity was only slightly influenced by a phosphine : rhodium ratio varying from 3.6 : 1 to 12 : 1. Further confirmation that the metal was strongly bound to the dendrimer came from ^{31}P NMR studies of solutions prepared from [Rh(acac)(CO)$_2$] and G1-16ethylPPh$_2$ (1 : 3) under CO and H$_2$ at atmospheric pressure. Two resonances were observed at room temperature, one (δ 37 ppm) for phosphine species bound to rhodium complexes and the other from the free phosphorus atoms (G1-16ethylPPh$_2$ resonates at δ −9.5 ppm). Both resonances were very broad (width at half maximum = 470 and 88 Hz, respectively). This is possibly because of different binding environments for the rhodium since the spectrum is the same in different solvents (CH$_2$Cl$_2$, THF) and the linewidth at half maximum of the signal from the unbound P atoms only changes slightly between −40 (63 Hz) and + 60 °C (150 Hz). This shows that the rhodium was not migrating rapidly around the surface of the dendrimer, nor dissociating on the NMR timescale, although the broadening of the signal on heating may suggest some slow exchange. The resonance from the Rh-bound phosphines appeared as two broad overlapping doublets (δ 37 and 36 ppm) at −40 °C, but as a single broad doublet (δ 37 ppm, $J_{P-Rh} \approx$ 130 Hz) at +60 °C, suggesting fluxionality within the bound complex, or that two coordination environments are present at low temperature. Two broad hydride signals were observed at δ −10.5 ppm (width at half maximum = 80 Hz) and −9.5 ppm (ratio 5: 1) in the ^{1}H NMR spectrum at room temperature. It is difficult to assign such signals to any configuration of rhodium complexes since the broad signal could arise from the presence of several different

species although a comparison with spectra obtained for $PEtPh_2$ complexes of rhodium is instructive.

In HP NMR and HP IR studies of $[Rh_2(\mu\text{-}OMe)_2(cod)_2]$ and $PEtPh_2$ under CO and H_2 pressure[42,43] Freixa *et al*. assigned the ^{31}P NMR resonance at δ_P 31.2 ppm (doublet) to the diphosphine ligand in a trigonal bipyramidal geometry (equatorial–equatorial (**C**) and equatorial–axial (**D**) isomers, Fig. 4), while

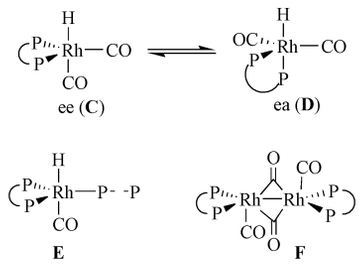

Fig. 4 Equatorial–equatorial (ee) ⇌ equatorial–axial (ea) equilibrium for trigonal bipyramidal hydridorhodium complexes together with the proposed tris(phosphine) and dimeric rhodium complexes.

the hydride region of the ^1H NMR showed a signal (td) at δ_H −9.3 ppm (P : Rh = 2 : 1 to 4 : 1, 30 bar H_2/CO).[42] The phosphorus atoms of the dimeric rhodium species (**F** in Fig. 4) resonated (^{31}P NMR) between δ_P 20.3 and 14.0 ppm. In another study (P : Rh = 4 : 1, 20 bar H_2, 4 bar CO, [Rh] = 0.024 mol dm^{-3}), Claver, van Leeuwen and co-workers[43] assigned a new ^{31}P NMR resonance at δ_P 34.5 ppm to the tris(phosphine) rhodium hydride (**E**, Fig. 4) with a ^1H NMR resonance for the hydride at δ_H −10.1 ppm. The extrapolation of these previous studies to this dendritic system would suggest that the complex did not form a dinuclear species (**F** in Fig. 4) under an atmosphere of H_2/CO, a configuration expected under low pressure of H_2.[1] It would be also tempting to assign the broad ^{31}P and ^1H NMR signals (at 37 and −10.5 ppm respectively) to **E** (Fig. 4**)** and the weak resonance in the ^1H NMR spectrum at −9.5 ppm to the equatorial and axial isomers of $RhH(CO)_2$(P–P), **C** and **D** (Fig. 4) where P–P is the dendrimer acting as a bidentate ligand. If this is the case, the ^{31}P NMR resonances of the bound phosphines in **C**/**D** and in **E** must overlap; we note that for $PEtPh_2$, they only differ by 3.3 ppm. The different environment of the phosphorus atoms and the number of combinations (between arms) would give a multitude of disturbed geometries to the rhodium/phosphine complexes, leading to the observed broad resonances. However, since a low pressure of CO/H_2 (*ca*. 1 atmosphere) and a different concentration of rhodium were used, it is difficult to extrapolate the results to the species present under catalytic conditions. In addition, comparison of the integration of the ^{31}P NMR signal of the free phosphines and coordinated phosphines suggests that only two phosphine species were coordinated to the metal centre (P : Rh = 4 : 1 in solution).

Because the infrared timescale allows the observation of the CO stretching vibrations of the two possible catalyst precursors, the ee and ea isomers of $[RhH(CO)_2(P)_2]$, we carried out HP IR studies on the dendrimer bound rhodium complexes. Since the rhodium–hydride bands are usually weak and hidden behind the CO absorption bands,[1] four absorption bands should be observed if both isomers are present. However, if a tris(phosphine) rhodium complex is formed only one or two bands are expected.[43] The HPIR spectroscopy study was carried out using $[Rh(CO)_2(acac)]$ (0.02 mol dm^{-3}) and G1-16ethylPPh$_2$ (P : Rh = 4 : 1) in toluene (10 cm^3) at 20 bar of H_2/CO at various temperature (25 to 100 °C) (Fig. 5 and Table 7). Interestingly at 25 °C three absorption bands at 2030, 1979 and 1954 cm^{-1} and a shoulder around 1940 cm^{-1} were visible indicating that the ee and ea isomers were already present when one would normally expect the formation of a dimeric species.[42,43] The comparative positions for the ea and ee isomers of $[RhH(CO)(PEtPh_2)_2]$ are 2037, 1990, 1979 and 1947 cm^{-1}, so

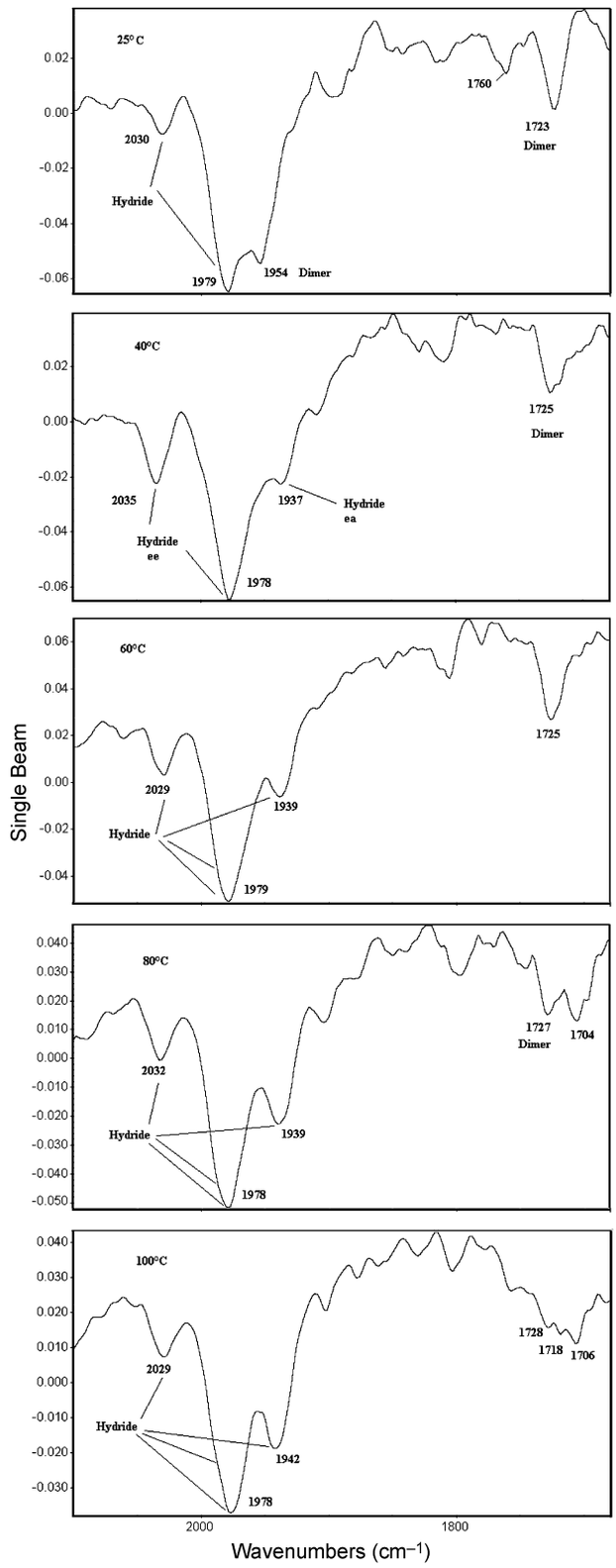

Fig. 5 HP IR of the rhodium/G1-16ethylPPh$_2$ complexes under 20 bar of H_2/CO at 25–100 °C.

Table 7 Selected IR absorption bands of rhodium/G1-16ethylPPh$_2$ complexes under 20 bar of H_2/CO

T/°C	ν_{CO} (ee)/cm^{-1}	ν_{CO} (ea)/cm^{-1}	ν_{CO} dimer/cm^{-1}
25	2030, 1979	Hidden, 1940	1954, 1723
40	2035, 1978	1990, 1937	1725
60	2029, 1979	1990, 1939	1725
80	2032, 1978	1990, 1939	1727
100	2029, 1978	1990, 1942	1728

the bands are assigned as in Table 7, which also shows the effect of temperature on the various bands. At 25 °C there are also weak absorptions near 1760 and 1725 cm^{-1}, which are assigned to the bridging carbonyls of the dimer (**F**, Fig. 4) which will also have a band near 1950 cm^{-1}. The absorptions assigned to the dimer become less significant on heating and there is little evidence for the presence of the tris-phosphine species under these high pressure conditions. By comparison with $PEtPh_2$, a single peak near 1978 cm^{-1} would be expected for this complex. The formation of a dicationic bimetallic Rh^{II} species as described by Stanley and co-workers can be ruled out since higher energy absorption bands would be expected (2095 to 2058 cm^{-1}).[41] On heating, the changes shown in Fig. 5 and Table 7 occur, suggesting that the dimer becomes less significant.

van Leeuwen and co-workers have investigated[44] the HP IR spectra of a number of thiaxantphos (P–P) complexes with different electron withdrawing and donating groups, which have different ratios of the ee and ea isomers of $[RhH(CO)(P–P)_2]$ and have published the spectra at 80 °C and 20 bar. Although our spectra are broader than his and there is overlap of the two bands between 1975 and 1990 cm^{-1}, a visual comparison of the relative intensities of the bands at 2030 (ν_{sym} for the ee isomer) and 1939 cm^{-1} (ν_{asym} for the ea isomer) shows that the spectrum is most similar to that of the hydridorhodium complexes containing thiaxantphos with *p*-Cl or *p*-F substituents on each of the phenyl groups attached to P, for which 75–90% of the complexes are present as the ee isomer, as determined from coupling in the hydride resonance of the ^1H NMR spectrum. This suggests that there is also a similar preference for ee binding by the dendrimer, which could help to account for the high selectivity to linear aldehydes in hydroformylation reactions. However, in the same study of thiaxantphos ligands, van Leeuwen and co-workers have shown that the ee : ea ratio does not entirely determine the hydroformylation selectivity. The natural bite angle seems to be more important and this has been attributed to the ability of the ligand to span transoid positions of the basal plane of the square pyramidal intermediate formed during alkene coordination.[44]

Molecular dynamics simulations of the dendrimers

In order to try to investigate further whether the higher l : b ratios observed with the dendrimer bound catalysts might in part be attributed to the natural bite angle, we carried out some molecular dynamics simulations of the G1-16ethylPPh$_2$ dendrimer ($Si_8O_{12}[CH_2CH_2SiMe(CH_2CH_2PPh_2)]_8$) using the Discover program contained in the Materials Studio Suite of Molecular Simulations Inc.[45] A molecular model from this work is shown in Fig. 6.

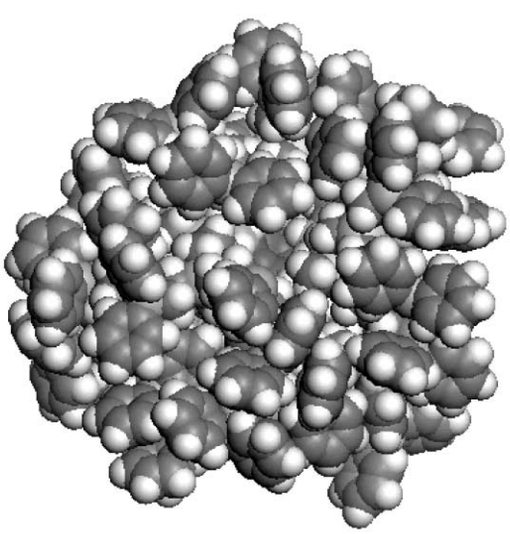

Fig. 6 Molecular model of the G1-16ethylPPh$_2$ dendrimer.

The results of the molecular dynamics simulations indicate that even the 1st generation G1-16ethylPPh$_2$ dendrimer is relatively globular in nature. Almost all of the diphenylphosphine groups are located on the external surface of the molecule, where they are available for binding to Rh. However, the bulkiness of such a species is evident and the high concentration of phosphine molecules at the surface explains the difficulty in achieving complete conversion of all arms of G1-16ethylPPh$_2$ and especially the G1-24ethylPPh$_2$.

The distribution of the P–P distances in the free ligands was then calculated from the final frames of the simulation for BISBI, Xantphos, and G1-16ethylPPh$_2$ and are shown in Fig. 7.

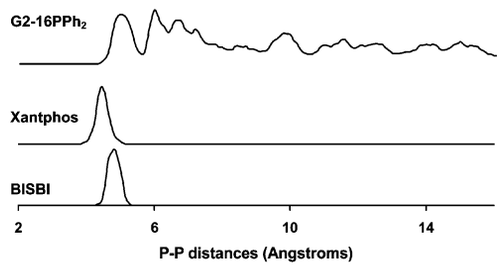

Fig. 7 P–P distances in different bidentate phosphorus ligands.

BISBI and Xantphos have P–P distances centered around 4.5 and 4.8 Å respectively, the molecular modelling of the dendrimer showed that within one arm, the P atoms were separated by 4–7 Å, whilst between arms there were always some distances in the 5–10 Å region. Rh–P distances are of the order of 2.5 Å.

The high regioselectivity observed using BISBI or Xantphos type ligands has been attributed to their ability to coordinate rhodium so as to give predominantly equatorial–equatorial (ee) coordination in key trigonal bipyramidal intermediates. Since there are many P–P separations for the dendrimer that are very similar to the P–P separations in BISBI and Xantphos (Fig. 7), it seems plausible that the crowding of the dendrimer surface gives a natural bite angle for many of the possible diphosphines formed very close to that required for ee binding and hence highly regioselective hydroformylation.

Models of the small molecules showed that the lowest energy configurations had the phosphine groups as far away from each other as possible. Assuming that the selectivity of the reaction depends to some degree on the amount of steric crowding at the surface of the dendrimer, one might expect that the compound tetra(diphenylphosphinoethyl)silane for which an X-ray crystal structure showed that the P atoms are 6.94 and 8.33 Å apart (Fig. 8), might show intermediate behaviour between

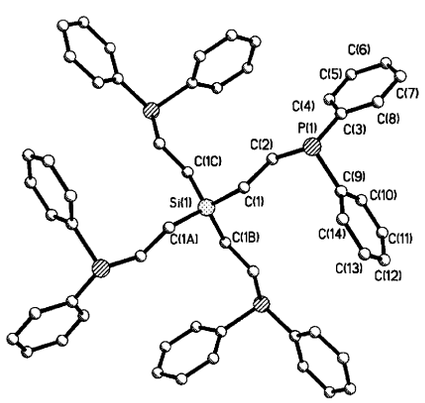

Fig. 8 X-Ray crystal structure of $Si(CH_2CH_2PPh_2)_4$.

G1-16ethylPPh$_2$ and diphenylphosphinodimethylsilane. Indeed this was confirmed since a l : b ratio of 5.2 : 1 was found.

It is important to remember that simulations of this kind are

very simplistic, and tell us nothing about the catalytic species. All they tell us is that the G1-16ethylPPh$_2$ dendrimer has possible configurations that lead to similar P–P distance distributions to other highly selective ligands. More advanced calculations, which are difficult on such large molecules, are needed if we are to elucidate details of the Rh-bound species. Molecular modelling studies of the other dendrimers are currently being carried out and will be reported separately.

Conclusion

POSS-based dendritic ligands functionalized with diphenylphosphine (G1-16ethylPPh$_2$ and G2-propyl-48ethylPPh$_2$) lead to high selectivity to the linear aldehyde (86%, l : b ratios up to 14 : 1) during the hydroformylation of terminal alkenes. Small molecule analogues (**1**, **2**, and **3**) did not show such selectivity indicating that a 'positive dendritic effect' is occurring.

It also appeared that only one dendritic framework (spacer of five atoms ($CH_2CH_2SiCH_2CH_2$) between the P atoms) led to high selectivity. It is tentatively concluded that other structures were either too compact (G1-16methylPPh$_2$, three atom spacers) or not sufficiently constrained (G1-16ethoxyPPh$_2$ and G1-16propylPPh$_2$, seven atom spacers) to give a high regioselectivity to the linear aldehyde. The seven atom spacers gave better selectivity than the three atom spacers. Interestingly the 2nd generation dendrimer, G2-propyl-48ethylPPh$_2$, with a similar structure to that of the G1-16ethylPPh$_2$ (five atoms between the P atoms) maintained a high selectivity (83.8%, l : b = 11.5) although leading to lower reactivity (rate *ca.* half). The composition of the dendritic framework was also important since, when replacing a carbon atom by an oxygen atom β to the phosphorus atoms (from G1-16ethylPPh$_2$ to G1-16methoxyPPh$_2$) the selectivity dropped. It is believed that the low selectivity could arise from a different geometry of the rhodium/dendritic ligand. Indeed an electronic effect is unlikely in this case since no such effect was found in the dendrimers with a seven atom spacer (G1-16ethoxyPPh$_2$ and G1-16propylPPh$_2$). The functionalization of the dendritic ligand with electron withdrawing groups (G1-16ethylPAr$_2$, Ar = 3,5-($C_6H_3(CF_3)_2$) led to lower selectivity.

The characterization of the rhodium complexes present in solution under H_2 and CO pressure was carried out using ^{1}H and ^{31}P NMR and HP IR techniques. It appeared that the species formed under H_2/CO was mainly the five-coordinated hydridorhodium complex (trigonal bipyramidal structure) with the ea and ee isomers in equilibrium, with the ee isomer predominating. The presence of the ea coordination may help to explain the low selectivity obtained when the POSS dendrimer was functionalized with more electron withdrawing arylphosphine species (G1-16ethylPAr$_2$), since Casey and coworkers have shown that electron withdrawing substituents increase the selectivity if they are on an equatorial P atom, but decrease it if they are on an axial P atom.[27] It may also be that the increased steric crowding provided by the presence of the fluorinated substituents prevents the P atoms from attaining the optimum relative disposition for obtaining high selectivity.

The presence of a tris(phosphine) rhodium complex was not completely ruled out for G1-16ethylPPh$_2$, but no strong evidence for the formation of active dimeric species could be found at temperatures above 25 °C. It is therefore believed that the high regioselectivity obtained with the G1-16ethylPPh$_2$ ligand is mainly due to the formation of a constrained bidentate ligand as in BISBI or Xantphos ligands. Molecular modelling studies tend to support this conclusion, since they show that many of the P–P distances in the G1-16ethylPPh$_2$ dendrimer, but not in the small molecules, are very similar to those found for BISBI and Xantphos, ligands that give high regioselectivity because they promote ee rather than ea binding of the bidentate ligand in key five-coordinate intermediates.

Experimental

Microanalyses were carried out by the University of St. Andrews Microanalysis service on a Carlo Erba 1110 CHNS analyser. NMR spectra were recorded on a Bruker AM 300 or a Varian 300 NMR spectrometer. The ^{1}H and ^{13}C NMR spectra were recorded with reference to tetramethylsilane (external). ^{31}P NMR spectra were referenced externally to 85% H_3PO_4. ^{13}C and ^{31}P NMR spectra were recorded with broad band proton decoupling. Infrared spectra were recorded using either a Perkin-Elmer 1710 or a Nicolet 460 Protege FTIR spectrometer. The high pressure infrared studies were carried out in a cylindrical internal reflectance cell. GC analyses were carried out using a Phillips PU4000 fitted with a capilliary column with nitrogen as the carrier gas. GCMS analyses were carried out using a Hewlett Packard 5890 GC interfaced with an Incos quadrupole mass spectrometer fitted with a SGE BP1 column or using a Hewlett Packard HP6890 GC with a 5973 mass selective detector fitted with a 5% phenyl methyl siloxane capilliary column. Matrix assisted laser desorption/ionisation (MALDI) mass spectra were obtained using a micromass TOF Spec 2E mass spectrometer system equipped with a 337 nm N_2 laser operating in positive ion reflection mode. Samples were prepared by addition of the matrix (α-cyano-4-hydroxycinnamic acid, 2.6-dihydroxyacetophenone, or 2,5-dihydroxybenzoic acid). The mixtures were then dissolved in a suitable solvent (THF or CH_2Cl_2) before being transferred to the sample holder and dried. All mass measurements refer to peaks for the most common isotopes (^{1}H, ^{12}C, ^{16}O, ^{29}Si, ^{31}P). NMR studies were carried out using solutions containing [Rh(acac)(CO)$_2$] (0.06 mol dm^{-3}) and the dendrimer (P : Rh = 4 : 1).[46] High pressure IR experiments were carried out as previously described using solutions containing [Rh(acac)-(CO)$_2$] (0.02 mol dm^{-3}) and the dendrimer (P : Rh = 4 : 1).[46]

All manipulations were carried out under dry, deoxygenated (Cr^{II} on silica) argon, using standard Schlenk line and catheter tubing techniques. Solvents were degassed before use having been dried by distillation from sodium diphenyl ketyl (THF, diethyl ether, light petroleum (boiling range 40–60 °C)), sodium (toluene, cyclohexane), CaH_2 (CH_2Cl_2) or magnesium alkoxide (methanol, ethanol). Water was distilled and stored under argon. Deuteriated solvents (Cambridge Isotope Laboratories) were degassed by repeated freeze–pump–thaw cycles and stored under argon over molecular sieves. Compounds were purchased from Aldrich, Acros or Strem and were used without further purification. G0-8vinyl,[26] G1-16vinyl,[17] G1-24Cl,[26] G1-24vinyl[26] and G2-propyl-48vinyl[17] were prepared by standard literature methods.

Molecular modelling was carried out using the Discover program contained in the Materials Studio Suite of Accelrys Inc.[45] Molecular dynamics were performed using the consistent valence force field (CVFF). The dendrimers were drawn using the draw facility on the Materials Studio viewer and minimized using steepest descent/conjugate gradient methods to a maximum energy derivative of less than RMS 0.001 kcal mol^{-1} Å^{-1}, relaxing bond lengths to their equilibrium distances. The models were then subjected to the heating and annealing process designed to reach a global minimum of energy for the structure. The structures were first heated to 1000 K to facilitate full expansion of the branches with a time step of 1 fs, and then annealed by reducing the temperature in 50 K steps for 5 ps dynamics down to 50 K. At 50 K the structures were again minimized to a maximum energy derivative of less than 0.001 kcal mol^{-1} Å^{-1} and allowed to equilibrate at 273 K for 600 ps. Every 1000th configuration of the structure was saved in full for analysis. The final 500 ps (500 frames) of the equilibration trajectory was used for analysis.

Syntheses

1,3,5,7,11,13,15-Octakis{2-[bis(2-diphenylphosphinoethyl)-methylsilyl]ethyl}pentacyclo[9.5.1.1^{3,9}.1^{5,15}.1^{7,13}]octasiloxane (G1-16ethylPPh$_2$). G1-16vinyl (0.25 g, 0.176 mmol) was added to a dry 20 cm^3 round bottomed Schlenk flask. AIBN (0.0078 g) was added and the flask was charged with cyclohexane (5 cm^3) and diphenylphosphine (2.1 g, 11.3 mmol). The flask was sealed and heated to 60 °C for 10 days. The resulting solution was allowed to cool and concentrated *in vacuo*. The excess phosphine was removed by vacuum distillation (120 °C, 0.1 mmHg) (Yield 0.73 g, 95%) or the product was loaded into a silica gel column (eluent: gradient of petroleum/diethyl ether) (Yield 0.66 g, 85%). The resulting crude product was a colourless low melting point solid (conversion >99%, compound **B**). MALDI-TOF: multiplets (mass increment of 16, oxidation) centered at *m*/*z* 4582 (large multiplet); 4299 (major multiplet); 4113 (medium multiplet); 3830 (br, small); 3628 (br, very small) corresponding respectively to 16, 15, 14, 13, 12 substituted arms ([M − *n*{PPh$_2$}], *n* = 0, 1, 2, 3, 4) (*m*/*z* expected 4397.9). The peaks at *m*/*z* 4582, 4299 and 4113 correspond to the molecule with 11, 5 and 0 phosphine species oxidised, respectively. The MALDI-TOF spectrum of the partially substituted compound **A** gave a broad signal centered at *m*/*z* 3680 (*ca.* 12 arms substituted). Microanalysis found for compound **B**: C, 67.9; H, 6.4. $C_{248}H_{280}O_{12}P_{16}Si_{16}$ requires C, 67.7; H, 6.4%. ^{31}P-{^{1}H} NMR ($CDCl_3$) δ_P (ppm) −9.4, −9.5, −14.4 (weak). ^{1}H NMR ($CDCl_3$) δ_H (ppm) 7.40–7.20 (br m, 160 H, P(C_6H_5)$_2$), 1.86 (br m, 32 H, PCH_2), 0.64–0.32 (m, 64 H, Si–CH_2), −0.16 (br, 24 H, Si–CH_3). ^{13}C-{^{1}H} NMR ($CDCl_3$): δ_C (ppm) 139.27 (d, J_{C-P} = 14.7 Hz, P(C_6H_5), C–P), 139.18 (d, J_{C-P} = 14.7 Hz, C–P), 132.80 (d, J_{C-P} = 18.8 Hz, C *ortho*), 132.70 (d, J_{C-P} = 17.4 Hz, C *ortho*), 128.55 (s, C *para*), 128.45 (d, $^1J_{C-P}$ = 6.71 Hz, C *meta*), 21.40 (d, $^1J_{C-P}$ = 14.8 Hz, CH_2P), 8.30 (d, $^2J_{C-P}$ = 12.1 Hz, $SiCH_2CH_2P$), 4.78 ($O_3SiCH_2CH_2$), 4.24 ($O_3SiCH_2CH_2$), −6.08 ($SiCH_3$).

1,3,5,7,11,13,15-Octakis{2-[tris(2-diphenylphosphinoethyl)-silyl]ethyl}pentacyclo[9.5.1.1^{3,9}.1^{5,15}.1^{7,13}]octasiloxane (G1-24ethylPPh$_2$). G1-24vinyl (0.245 g, 0.162 mmol) was added to a dry 20 cm^3 round bottomed Schlenk flask. AIBN (0.0078 g) was added and the flask was charged with cyclohexane (7 cm^3) and diphenylphosphine (2.90 g, 0.0156 mol). The flask was sealed and heated to 60 °C for 10 days. The resulting solution was allowed to cool and the excess phosphine was removed by vacuum distillation (120 °C, 0.1 mmHg). The resulting crude product was a white solid (Yield 0.65g, 95% for a conversion of 60%). ^{31}P-{^{1}H} NMR (CD_2Cl_2) δ_P (ppm) −9.5 (br). ^{1}H NMR ($CDCl_3$) δ_H (ppm) 7.7–7.2 (br m, 140 H, P(C_6H_5)$_2$), 6.1–5.8 (br, 20 H, CH=CH_2), 5.7–5.5 (br, 10 H, CH=CH_2), 2.2–1.8 (br, 28 H, PCH_2), 0.90–0.25 (br, 60 H, $SiCH_2$). IR/cm^{-1} (KBr disc) 2956s, 2919s, 2873s, 1455vs, 1409vs (PCH_2), 1260vs ($SiCH_2$), 1120vs ($SiCH_2CH_2Si$), 1040vs (SiOSi), 952s, 800m, 750vs, 707vs.

1,3,5,7,11,13,15-Octakis{2-{tris{3-[bis(2-diphenylphosphino-ethyl)methylsilyl]propyl}silyl}ethyl}pentacyclo[9.5.1.1^{3,9}.1^{5,15}.-1^{7,13}]octasiloxane (G2-propyl-48ethylPPh$_2$). G2-propyl-48vinyl (0.22 g, 5.2 × 10^{-5} mol) was added to a dry 20 cm^3 round bottomed Schlenk flask. AIBN (0.008 g) was added and the flask was charged with cyclohexane (5 cm^3) and diphenylphosphine (1.86 g, 0.01 mol). The reaction mixture was heated to 50 °C for 12 days. The resulting solution was allowed to cool and taken to dryness *in vacuo*. The product was loaded into a silica gel column (eluent: gradient of petroleum/diethyl ether). The isolated product was a colourless low melting point solid (0.443 g, yield 75% for a conversion of 84%). ^{31}P-{^{1}H} NMR ($CDCl_3$) δ_P (ppm) −9.9 (br). ^{1}H NMR ($CDCl_3$) δ_H (ppm) 7.6–7.0 (br m, 408 H, P(C_6H_5)$_2$), 6.2–5.8 (br, 14 H, CH=CH_2), 5.65–5.45 (br, 7 H, CH=CH_2), 1.86 (br, 82 H, PCH_2), 1.62 (br, CH_2), 1.45–1.00 (br, CH_2), 1.00–0.20 (br, $SiCH_2$), 0.20 to −0.20 (br, 72 H, Si–CH_3). ^{13}C-{^{1}H} NMR ($CDCl_3$): δ_C (ppm) 139.27 (d, J_{C-P} = 14.7 Hz, P(C_6H_5), C–P), 139.18 (d, J_{C-P} = 14.7 Hz, P(C_6H_5), C–P), 137.0 (CH_2, Si-vinyl), 132.8 (d, J_{C-P} = 18.8 Hz, C *ortho*), 132.70 (d, J_{C-P} = 18.0 Hz, C *ortho*), 128.50 (s, C *para*), 128.45 (d, J_{C-P} = 6.7 Hz, C *meta*), 21.50 (d, $^1J_{C-P}$ = 14.2 Hz, CH_2P), 18.52, 16.89, 9.07 (d, $^2J_{C-P}$ = 12.0 Hz, $SiCH_2CH_2P$), 4.57 (br, $O_3Si-CH_2CH_2$), −5.38 ($SiCH_3$).

1,3,5,7,11,13,15-Octakis{2-{bis{bis-2-[bis(3,5-trifluoromethyl)-phenyl]phosphinoethyl}methylsilyl}ethyl}pentacyclo[9.5.1.1.1^{3,9}.-1^{5,15}.1^{7,13}]octasiloxane (G1-16ethylPAr$_2$). G1-16vinyl (0.25 g, 0.176 mmol) was added to a dry 20 cm^3 round bottomed Schlenk flask. AIBN (0.0078 g) was added and the flask was charged with cyclohexane (5 cm^3) and [3,5-$(CF_3)_2C_6H_3]_2PH$ [27] (3.87 g, 8.45 mmol). The flask was sealed and heated to 60 °C for 30 days. The resulting solution was allowed to cool and the excess phosphine was removed by vacuum distillation (140 °C, 0.02 mmHg) to give a colourless solid (1.17 g, yield 96% for a conversion of 75%). MALDI-TOF: *m*/*z*: 6919, 6459, 6001 (major), 5543 (major), 4988 (respectively 12, 11, 10, 9, 8 arms substituted). Other peaks at *m*/*z* 6365, 5905, 5446, 4891 (fragmentation). ^{31}P-{^{1}H} NMR ($CDCl_3$) δ_P (ppm) −6.6, −6.9, −7.0, −12.9. ^{1}H NMR ($CDCl_3$) δ_H (ppm) 8.2–7.8 (m, 72 H, P($C_6H_3(CF_3)_2$)$_2$), 6.0 (br, 24 H, CH=CH_2), 5.7 (br, 12 H, CH=CH_2), 2.1 (br, 24 H, PCH_2), 1.0–0.4 (br m, 56 H, Si–CH_2), 0.6 (br, 24 H, Si–CH_3). ^{13}C-{^{1}H} NMR ($CDCl_3$): δ_C (ppm) 140.60 (m, C quaternary), 135.75, 133.80, 132.73, 132.50, 125.00, 124.66, 123.63, 121.39, 110.16, 21.34 ($SiCH_2CH_2P$), 8.30 ($SiCH_2CH_2P$), 5.20 ($O_3SiCH_2CH_2$), 4.33 ($O_3SiCH_2CH_2$), −6.08 ($SiCH_3$).

Bis(diphenylphosphinoethyl)dimethylsilane. Dimethyldivinylsilane (0.267 g, 2.39 mmol) was added to a dry 20 cm^3 round bottomed Schlenk flask. AIBN (0.0078 g) was added and the flask was charged with toluene (5 cm^3) and diphenylphosphine (2.675 g, 14.3 mmol). The flask was sealed and heated to 60 °C for 4 hours. The resulting solution was allowed to cool and taken to dryness *in vacuo*. The excess phosphine was removed by vacuum distillation (120 °C, 1.0 mmHg). The product was recrystallised from petroleum to give a white crystalline solid (1.06 g, 92%). Microanalysis found C, 74.0; H, 7.0. $C_{30}H_{34}P_2Si$ requires C, 74.4; H, 7.1%. ^{31}P-{^{1}H} NMR ($CDCl_3$) δ_P (ppm) −9.4. ^{1}H NMR ($CDCl_3$) δ_H (ppm) 7.42–7.30 (m, 20 H, P(C_6H_5)$_2$), 1.94 (m, 4 H, PCH_2), 0.60 (m, 4 H, Si–CH_2), −0.16 (br, 6 H, Si–CH_3). ^{13}C-{^{1}H} NMR ($CDCl_3$): δ_C (ppm) 138.95 (d, J_{C-P} = 17.6 Hz, C–P), 132.90 (d, J_{C-P} = 17.5 Hz, C *ortho*), 128.70 (d, $^1J_{C-P}$ = 6.71 Hz, C *meta*), 128.46 (C *para*), 21.62 (d, $^1J_{C-P}$ = 13.4 Hz, CH_2P), 10.40 (d, $^2J_{C-P}$ = 9.40 Hz, $SiCH_2CH_2P$), −3.78 ($SiCH_3$).

Tetrakis(2-diphenylphosphinoethyl)silane [ref. 33]. Tetravinylsilane (0.20 g, 1.47 mmol) was added to a dry 20 cm^3 round bottomed Schlenk flask. AIBN (0.0078 g) was added and the flask was charged with toluene (5 cm^3) and diphenylphosphine (2.73 g, 14.7 mmol). The flask was sealed and heated to 60 °C for 4 hours. The resulting solution was allowed to cool and taken to dryness *in vacuo*. The excess phosphine was removed by vacuum distillation (120 °C, 1.0 mmHg). The product was recrystallised from hot dichloromethane to give a white crystalline solid (1.20 g, 93%). Microanalysis found C, 76.0; H, 6.10. $C_{56}H_{56}P_4Si$ requires C, 76.3; H, 6.4%. ^{31}P-{^{1}H} NMR ($CDCl_3$) δ_P (ppm) −9.48. ^{1}H NMR ($CDCl_3$) δ_H (ppm) 7.33 (br m, 40 H, P(C_6H_5)$_2$), 1.79 (br m, 8l H, PCH_2), 0.61 (br m, 8 H, Si–CH_2). ^{13}C-{^{1}H} NMR ($CDCl_3$): δ_C (ppm) 138.95 (d, J_{C-P} = 17.6 Hz, P(C_6H_5), C–P), 132.90 (d, J_{C-P} = 17.5 Hz, C *ortho*), 128.70 (d, $^1J_{C-P}$ = 6.7 Hz, C *meta*), 128.46 (s, C *para*), 21.62 (d, $^1J_{C-P}$ = 13.4 Hz, CH_2P), 10.40 (d, $^2J_{C-P}$ = 9.4 Hz, $SiCH_2CH_2P$).

1,3,5,7,11,13,15-Octakis{2-[tris(diphenylphosphinomethyl)-silyl]ethyl}pentacyclo[9.5.1.1.1^{3,9}.1^{5,15}.1^{7,13}]octasiloxane (G1-24methylPPh$_2$). $LiCH_2PPh_2$/TMEDA [30] (0.741 g, 2.22 mmol) was dissolved at −78 °C in a Schlenk flask containing THF

(20 cm^3). The solution was transferred *via* cannula to a Schlenk flask containing G1-24Cl (0.15 g, 0.0874 mmol) in THF (10 cm^3). The mixture was stirred for 60 h. The solvent was removed *in vacuo*. Dichloromethane was added (20 cm^3). After settling overnight, the liquid was transferred *via* cannula and taken to dryness *in vacuo*. The product was washed with diethyl ether (3 × 10 cm^3) and dried *in vacuo*. The resulting product was a white solid (0.44 g, conversion 70%, yield 93%). MALDI-TOF: broad peak centered at *m/z* 4678 (*ca.* 17 arms substituted) (*m/z* expected 5646.8). ^{31}P-{^{1}H} NMR (CD_2Cl_2) δ_P (ppm) −23.9. ^{1}H NMR (CD_2Cl_2) δ_H (ppm) 7.5–6.6 (m, 240 H, C_6H_5), 1.03 (s, 48 H, –CH_2P), 0.9–0.4 (m, 32 H, Si–CH_2CH_2-Si). ^{13}C-{^{1}H} NMR (CD_2Cl_2) δ_C (ppm) 141.3 (br, P-C), 132.7 (br, C *ortho*), 128.4 (br, C *para*, C *meta*), 11.6 (br, $SiCH_2P$), 5.0 (br, $SiCH_2CH_2Si$). IR/cm^{-1} (KBr disc) 3049vs (C=C), 2908m, 1584w (C=C), 1479s (C=C, PPh), 1433s ($SiCH_2P$), 1088vs ($SiCH_2CH_2Si$), 1025vs (SiOSi), 999s (PPh), 740s, 695s, 471m.

1,3,5,7,11,13,15-Octakis{2-[bis(diphenylphosphinomethyl)-methylsilyl]ethyl}pentacyclo[9.5.1.1^{3,9}.1^{5,15}.1^{7,13}]octasiloxane (G1-16methylPPh$_2$). $LiCH_2PPh_2$/TMEDA[47] (0.741 g, 2.22 mmol) (50% excess) was dissolved at −78 °C in a Schlenk flask containing THF (20 cm^3). The solution was transferred *via* cannula to a Schlenk flask containing G1-16Cl[17] (0.145 g, 0.0925 mmol) in THF (10 cm^3). The mixture was stirred for 4 days. The solvent was removed *in vacuo* and the solid mixture was loaded onto silica gel and eluted with a gradient of petroleum and diethyl ether. After evaporation under vacuum of the solvent, the product was obtained as a white solid (0. 262 g, conversion >95%, yield 70%). MALDI-TOF: *m/z* 4176 (*m/z* expected 4173.5), other peak at 4194 (1 oxide), 4036.5, 3992.3 (M − CH_2PPh_2), 3736.0. ^{31}P-{^{1}H} NMR ($CDCl_3$) δ_P (ppm) −22.6, −22.7. ^{13}C-{^{1}H} NMR ($CDCl_3$) δ_C (ppm) 141.50 (d, J_{C-P} = 12.7 Hz, C–P), 141.33 (d, J_{C-P} = 12.7 Hz, C–P), 133.03 (d, J_{C-P} = 19.6 Hz, C *ortho*), 132.78 (d, J_{C-P} = 17.2 Hz, C *ortho*), 128.56 (s, C *meta*, C *para*), 12.80 (d, J_{C-P} = 28 Hz, $SiCH_2P$), 7.97 (br, $SiCH_2CH_2SiO_{3/2}$), 5.00 (br, CH_3SiCH_2), −2.67 (br, $SiCH_3$). ^{1}H NMR ($CDCl_3$) δ_H (ppm) 7.4–7.0 (m, 160 H, C_6H_5), 1.21 (br, 32 H, –CH_2P), 0.75–0.45 (m, 32 H, Si–CH_2CH_2–Si), −0.36 (br, 24 H, $SiCH_3$). IR/cm^{-1} (KBr disc) 3049vs (C=C), 2908m, 1584w (C=C), 1479s (C=C, PPh), 1433s ($SiCH_2P$), 1088vs ($SiCH_2CH_2Si$), 1025vs (SiOSi), 999s (PPh), 740s, 695s, 471m.

1,3,5,7,11,13,15-Octakis{2-[bis(diphenylphosphinomethoxy)-methylsilyl]ethyl}pentacyclo[9.5.1.1^{3,9}.1^{5,15}.1^{7,13}]octasiloxane (G1-16methoxyPPh$_2$). $HPPh_2$ (1.2 cm^3, 9.96 mmol) and paraformaldehyde (0.2088 g) were heated in a Schlenk tube for 90 min at 120 °C to afford Ph_2PCH_2OH.[31] The compound formed *in situ* and NEt_3 (1.4 cm^3) in THF (20 cm^3) were added to a Schlenk flask containing G1-16Cl[17] (0.3223 g, 0.207 mmol) in THF (10 cm^3). The mixture was stirred for 4 days. The solvent was removed *in vacuo* and the solid mixture was loaded onto a silica column and eluted with a gradient of petroleum and diethyl ether. After evaporation under vacuum of the solvent, the product was obtained as a white solid (0.604 g, conversion >86%, yield 76%). MALDI-TOF: *m/z* 4432.3 (*m/z* expected 4429.8), other major peaks at 4448 (oxide), 4248 (M − {PPh_2}), 4234 (M − {CH_2PPh_2}), 4051 (M − 2{PPh_2}), 4037 (M − 2{CH_2PPh_2}), 3836 (M − 3{PPh_2}), 3819 (M − 3{CH_2PPh_2}), 3636 (M − 4{PPh_2}), 3622 (M − 4{CH_2PPh_2}). Microanalysis found C, 66.1; H, 6.3. $C_{232}H_{248}O_{28}P_{16}Si_{16}$ requires C, 62.9; H, 5.6%. ^{31}P-{^{1}H} NMR ($CDCl_3$) δ_P (ppm) −13.6 (br). ^{1}H NMR ($CDCl_3$) δ_H (ppm) 7.8–7.1 (m, 160 H, C_6H_5), 4.35 (br, OCH_2, 32 H), 0.80–0.35 (m br, 32 H, Si–CH_2CH_2–Si), −0.05 (br, 24 H, $SiCH_3$). ^{13}C-{^{1}H} NMR ($CDCl_3$) δ_C (ppm) 143.30 (br, phenyl P–C), 133.24 (d, J_{C-P} = 26.5 Hz, C *ortho*), 128.87 (s, C *para*), 128.64 (d, J_{C-P} = 6.71 Hz, C *meta*), 63.17 (br, OCH_2), 4.74 (br, $SiCH_2CH_2SiO_{3/2}$), 3.14 (br, $SiCH_2CH_2SiO_{3/2}$), −6.15 (br, $SiCH_3$).

1,3,5,7,11,13,15-Octakis{2-[bis(2-diphenylphosphinoethoxy)-methylsilyl]ethyl}pentacyclo[9.5.1.1^{3,9}.1^{5,15}.1^{7,13}]octasiloxane (G1-16ethoxyPPh$_2$). $Ph_2PCH_2CH_2OH$[32] (1.12 g, 4.9 mmol, 2.5 fold excess) and NEt_3 (0.75 cm^3) in THF (20 cm^3) were added to a Schlenk flask containing G1-16Cl (0.198 g, 0.128 mmol) in THF (10 cm^3). The mixture was stirred for 5 days. The solvent was removed *in vacuo* and the solid mixture was loaded onto a silica column where it was eluted with a gradient of petroleum and diethyl ether. After evaporation of the solvent under vacuum, the product was obtained as a white solid (0.48 g, conversion >92%, yield 85%). MALDI-TOF: *m/z* 4657.6 (*m/z* expected 4653.8), other major peaks at 4505; 4445.2 (M − {CH=CHPPh$_2$}), 4233.7 (M − 2{CH=CHPPh$_2$}), 4156, 4047, 3943. ^{31}P-{^{1}H} NMR ($CDCl_3$) δ_P (ppm) −22.3, −22.5. ^{1}H NMR ($CDCl_3$) δ_H (ppm) 7.6–7.3 (m, 160 H, C_6H_5), 3.84 (br d, $^3J_{P-H}$ = 7.6 Hz, OCH_2, 32 H), 2.4 (br d, $^2J_{P-H}$ = 7.7 Hz, 32 H, PCH_2), 0.75–0.55 (m, 32 H, Si–CH_2CH_2–Si), 0.02 (br, 24 H, $SiCH_3$). ^{13}C-{^{1}H} NMR ($CDCl_3$) δ_C (ppm) 141.4 (br, C–P), 132.90 (br, C *ortho*), 128.56 (s, C *meta*, C *para*), 60.54 (d, J_{C-P} = 26.5 Hz, CH_2P), 32.33 (d, J_{C-P} = 12.6 Hz, OCH_2), 7.97 (br, $SiCH_2CH_2SiO_{3/2}$), 5.00 (br, CH_3SiCH_2), −5.37 (br, $SiCH_3$).

1,3,5,7,11,13,15-Octakis{2-[bis(2-diphenylphosphinopropyl)-methylsilyl]ethyl}pentacyclo[9.5.1.1^{3,9}.1^{5,15}.1^{7,13}]octasiloxane (G1-16propylPPh$_2$). Magnesium turnings (0.50 g, 20.7 mmol) and $Ph_2PCH_2CH_2CH_2Cl$[33] (4.982 g, 18.96 mmol) were mixed in THF (20 cm^3). The mixture was heated to reflux and initiated with a small amount of reacting $BrCH_2CH_2Br$/Mg.[33] Heating and stirring were continued for 1 h. The mixture was filtered into a Schlenk flask containing G1-16Cl (0.615 g, 0.396 mmol) in THF (20 cm^3). The mixture was stirred for 4 days. The mixture was added to an aqueous solution of NH_4Cl (0.1 mol dm^{-3}). The organic phase was concentrated *in vacuo* and the residue was loaded onto silica gel where it was eluted with a gradient of petroleum and diethyl ether. After evaporation of the solvent under vacuum, the product was obtained as a non-crystalline solid (1.30 g, conversion >85% (^{1}H NMR), yield 75%). MALDI-TOF: *m/z* 3574.9 (unknown, fragmentation) (*m/z* expected 4623), other major peaks (unknown fragmentation) at 3426, 3365, 3153. Microanalysis found C, 63.3; H, 7.2. $C_{264}H_{312}O_{12}P_{16}Si_{16}$ requires C, 68.6; H, 6.8%. ^{31}P-{^{1}H} NMR ($CDCl_3$) δ_P (ppm) −16.1, −16.2, −16.4. ^{1}H NMR ($CDCl_3$) δ_H (ppm) 7.6–7.3 (m, 160 H, C_6H_5), 3.84 (br d, $^3J_{P-H}$ = 7.6 Hz, OCH_2, 32 H), 2.4 (br d, $^2J_{P-H}$ = 7.7 Hz, 32 H, PCH_2), 0.75–0.55 (m, 32 H, Si–CH_2CH_2–Si), 0.02 (br, 24 H, $SiCH_3$). ^{1}H NMR ($CDCl_3$) δ_H (ppm) 7.55–7.30 (m, 160 H, C_6H_5), 2.18 (br, 32 H, PCH_2), 1.60–1.40 (br, 32 H, CH_2), 0.88 (br, 32 H, $SiCH_2$), 0.80–0.55 (br, 32 H, $SiCH_2$), 0.15 (br, $SiCH_3$). ^{13}C-{^{1}H} NMR ($CDCl_3$) δ_C (ppm) 139.0 (br, P–C), 133.00 (d, J_{C-P} = 18.4 Hz, C *ortho*), 128.75 (s, C *para*), 128.70 (d, J_{C-P} = 5.8 Hz, C *meta*), 32.29 (br), 20.31 (d, J_{C-P} = 17.2 Hz, PCH_2), 18.16, 4.00 (br, $SiCH_2$), −2.10 (s, $SiCH_3$).

Catalytic reactions

The functionalised POSS dendrimer, the rhodium source ([$Rh_2(O_2CMe)_4$] or [$Rh(CO)_2$(acac)]) and ethanol or THF (4 cm^3) were charged into a Schlenk tube and stirred until complexation of the rhodium with the phosphine species was complete. The catalytic solution and substrate were then injected into a degassed autoclave heated under CO/H_2 (6 bar) to the reaction temperature for 1 h with stirring at 1000 rpm. The substrate was injected and the pressure of CO/H_2 (1/1) was increased to the desired pressure. The pressure was kept constant by feeding CO/H_2 through a mass flow controller from a ballast vessel (Pressure drop in ballast vessel monitored every 5 s). After reaction, the products were analysed by GC/MS or, for quantitative work using the same GC, but an FID detector.

X-Ray crystallographic structure determination of tetrakis-(2-diphenylphosphinoethyl)silane.[33]

$C_{56}H_{56}P_4Si$, colourless prism, 0.18 × 0.1 × 0.1 mm, tetragonal, space group *I*-4, $Z = 2$, $a = 20.4806(14)$, $c = 5.7429(6)$ Å, $V = 2408.9(3)$ Å^3, ρ_c 1.215 Mg m^{-3}, $2\theta_{max} = 46.62°$, graphite monochromated Mo-Kα radiation ($\lambda = 0.71073$ Å), μ(Mo-Kα) = 0.218 mm^{-1}, $T = 293$ K. Data were measured on a Bruker SMART CCD, and Lorentzian polarization and absorption (SADABS, max./min. transmission 1.0000/0.7616) corrections were performed. Of 6048 measured data, 1725 were unique ($R_{int} = 0.1057$) and 1090 observed [$I > 2\sigma(I)$]. The structure was solved by direct methods. The non-hydrogen atoms were refined anisotropically, the hydrogen atoms were idealized and refined isotropically using a riding model. Structural refinements were performed with the full-matrix least-squares method on F^2 for all data (G. M. Sheldrick, SHELXTL version 5.10, Bruker AXS, Madison WI, 1997) to give conventional $R_1 = 0.0453$ and $wR_2 = 0.0512$ for 139 parameters with residual electron extremes of 0.162 and −0.172 e Å^{-3}.

CCDC reference number 189436.

See http://www.rsc.org/suppdata/dt/b2/b206597e/ for crystallographic data in CIF or other electronic format.

Acknowledgements

We thank the University of St. Andrews for a studentship (L. R.). R. E. M. thanks the Royal Society for the provision of a University Research Fellowship.

References

1 P. W. N. M. van Leeuwen and C. Claver, *Rhodium Catalysed Hydroformylation*, Kluwer Academic Publishers, Dordrecht, 2000.
2 D. Astruc and F. Chardac, *Chem. Rev.*, 2001, **101**, 2991.
3 G. E. Oosterom, J. N. H. Reek, P. C. J. Kamer and P. W. N. M. van Leeuwen, *Angew. Chem., Int. Ed.*, 2001, **40**, 1828.
4 N. Brinkmann, G. Giebel, G. Lohmer, M. T. Reetz and U. Kragl, *J. Catal.*, 1999, **183**, 163.
5 D. de Groot, E. Eggeling, J. C. de Wilde, H. Kooijman, R. J. van Haaren, A. W. van der Made, A. L. Spek, D. Vogt, J. N. H. Reek, P. C. J. Kamer and P. W. N. M. van Leewen, *Chem. Commun.*, 1999, 1623.
6 N. J. Hovestad, E. B. Eggeling, H. J. Heidbüchel, J. T. B. H. Jastrzebski, U. Kragl, W. Keim, D. Vogt and G. van Koten, *Angew. Chem., Int. Ed.*, 1999, **38**, 1655.
7 C. P. Casey and L. M. Petrovich, *J. Am. Chem. Soc.*, 1995, **117**, 6007.
8 M. Kranenburg, Y. E. M. van der Burgt, P. C. J. Kamer, P. W. N. M. van Leeuwen, K. Goubitz and J. Fraanje, *Organometallics*, 1995, **14**, 3081.
9 A. W. Kleij, R. A. Gossage, J. T. B. H. Jastrzebski, J. Boersma and G. van Koten, *Angew. Chem., Int. Ed.*, 2000, **39**, 176.
10 R. Breinbauer and E. R. Jacobsen, *Angew. Chem., Int. Ed.*, 2000, **39**, 3604.
11 C. Francavilla, M. D. Drake, F. V. Bright and M. R. Detty, *J. Am. Chem. Soc.*, 2001, **123**, 57.
12 V. Maraval, R. Laurent, A.-M. Caminade and J.-P. Majoral, *Organometallics*, 2000, **19**, 4025.
13 P. Bhyrappa, J. K. Young, J. S. Moore and K. S. Suslick, *J. Mol. Catal. A: Chem.*, 1996, **113**, 109.
14 Y. H. Niu, L. E. Yeung and R. M. Crooks, *J. Am. Chem. Soc.*, 2001, **123**, 6840.
15 Q.-H. Fan, Y.-M. Chen, D.-Z. Jiang, X.-M. Chen, F. Xi and A. S. C. Chan, *Chem. Commun.*, 2000, 789.
16 T. Mizugaki, M. Murata, M. Ooe, K. Ebitani and K. Kaneda, *Chem. Commun.*, 2002, 52.
17 L. Ropartz, D. F. Foster, R. E. Morris, A. M. Z. Slawin and D. J. Cole-Hamilton, *J. Chem. Soc., Dalton Trans.*, 2002, 1997.
18 L. Ropartz, R. E. Morris, D. F. Foster and D. J. Cole-Hamilton, *Chem. Commun.*, 2001, 361.
19 L. Ropartz, R. E. Morris, G. P. Schwarz, D. F. Foster and D. J. Cole-Hamilton, *Inorg. Chem. Commun.*, 2000, **3**, 714.
20 L. Ropartz, R. E. Morris, D. F. Foster and D. J. Cole-Hamilton, *J. Mol. Catal.*, 2002, **182–183**, 99.
21 M. Reetz and D. Giebel, *Angew. Chem., Int. Ed.*, 2000, **39**, 2498.
22 A. J. Gong, Q. H. Fan, Y. M. Chen, H. W. Liu, C. F. Chen and F. Xi, *J. Mol. Catal. A: Chemical*, 2000, **159**, 225.
23 D. de Groot, P. G. Emmerink, C. Coucke, J. N. H. Reek, P. C. J. Kamer and P. W. N. M. van Leeuwen, *Inorg. Chem. Commun.*, 2000, **3**, 711.
24 P. Arya, G. Panda, N. V. Rao, H. Alper, S. C. Bourque and L. E. Manzer, *J. Am. Chem. Soc.*, 2001, **123**, 2889.
25 P. Arya, N. V. Rao, J. Singkhonrat, H. Alper, S. C. Bourque and L. E. Manzer, *J. Org. Chem.*, 2000, **65**, 1881.
26 P.-A. Jaffrès and R. E. Morris, *J. Chem. Soc., Dalton Trans.*, 1998, 2767.
27 C. P. Casey, E. L. Paulsen, E. W. Beuttenmueller, B. R. Proft, L. M. Petrovich, B. A. Matter and D. R. Powell, *J. Am. Chem. Soc.*, 1997, **119**, 11817.
28 C. P. Casey, E. L. Paulsen, E. W. Beuttenmueller, B. R. Proft, B. A. Matter and D. R. Powell, *J. Am. Chem. Soc.*, 1999, **121**, 63.
29 J. D. Unruh and J. R. Christenson, *J. Mol. Catal.*, 1982, **14**, 19.
30 D. J. Peterson, *J. Organomet. Chem.*, 1967, **8**, 199.
31 M. Slany, M. Bardaji, A.-M. Caminade, B. Chaudret and J.-P. Majoral, *Inorg. Chem.*, 1997, **36**, 1939.
32 D. Chantreux, J.-P. Gamet, R. Jacquier and J. Verducci, *Tetrahedron*, 1984, **40**, 3087.
33 E. Arpac and L. Dahlenburg, *Z. Naturforsch., Teil B*, 1980, **35**, 146.
34 A. Buhling, P. C. J. Kamer, P. vanLeeuwen, J. W. Elgersma, K. Goubitz and J. Fraanje, *Organometallics*, 1997, **16**, 3027.
35 W. Schalk, P. Wirth, G. E. M. Dannenberg and V. Schmied-Kowarzik, *Ger. Pat.*, 1118981, 1959.
36 K. J. Haxton, L. Ropartz, D. J. Cole-Hamilton and R. E. Morris, to be submitted.
37 D. Evans, J. A. Osborn and G. Wilkinson, *J. Chem. Soc. A.*, 1968, 3133.
38 D. Evans, G. Yagupsky and G. Wilkinson, *J. Chem. Soc. A*, 1968, 2660.
39 G. Gregorio, G. Montrasi, M. Tampieri, P. Cavalieri d'Oro, G. Pagani and A. Andreetta, *Chim. Ind. (Milan)*, 1980, **62**, 389.
40 M. E. Broussard, B. Juma, S. G. Train, W.-J. Peng, S. A. Laneman and G. G. Stanley, *Science*, 1993, **260**, 1784.
41 R. C. Matthews, D. K. Howell, W.-J. Peng, S. G. Train, W. D. Treleavan and G. G. Stanley, *Angew. Chem., Int. Ed. Engl.*, 1996, **35**, 2253.
42 Z. Freixa, M. Pereira, A. A. C. C. Pais and J. C. Bayón, *J. Chem. Soc., Dalton Trans.*, 1999, 3245.
43 I. del Rio, W. G. J. de Lange, P. W. N. M. van Leeuwen and C. Claver, *J. Chem. Soc., Dalton Trans.*, 2001, 1293.
44 L. A. van der Veen, M. D. K. Boele, F. R. Bregman, P. C. S. Kamer, P. W. N. M. van Leeuwen, F. Goubitz, J. Fraanje, H. Schenk and C. Bo, *J. Am. Chem. Soc.*, 1998, **120**, 11616.
45 Materials Studio Suite, Accelrys Inc., San Diego, 2000.
46 J. Rankin, A. C. Benyei, A. D. Poole and D. J. Cole-Hamilton, *J. Chem. Soc., Dalton Trans.*, 1999, 3771.
47 D. J. Peterson and H. R. Hays, *J. Org. Chem.*, 1965, **30**, 1939.